Transmission-Conversion Efficiency Maximization Technique for MIMO Wireless Power Transfer Systems in ISAC Applications

Young-Seok Lee, *Graduate Student Member, IEEE*, Taeyeong Yoon, *Graduate Student Member, IEEE*, Young Jin Song, *Graduate Student Member, IEEE*, Sun K. Hong, *Senior Member, IEEE*, Jungsuek Oh, *Senior Member, IEEE*, and Sangwook Nam, *Life Senior Member, IEEE*

***Abstract*—This letter presents a dc power optimization methodology for multiple-in–multiple-out (MIMO) wireless power transfer (WPT) systems especially for integrated sensing and communications (ISAC) applications. Given a rectifier that has already been optimized itself, the transmission-conversion efficiency (TCE) is optimized by jointly considering both RF–RF (air propagation) and RF–dc (rectifier) stages. In a specific MIMO WPT configuration with a 16 × 16 transmitter array and an 8 × 8 receiver array, simulation result showed a significant 65.6% TCE improvement over conventional RF-to-RF power transfer efficiency optimization. It can offer a boundary for future real-time WPT algorithms.**

***Index Terms*—Global optimization, power transfer efficiency (PTE), transmission-conversion efficiency (TCE), wireless power transfer (WPT).**

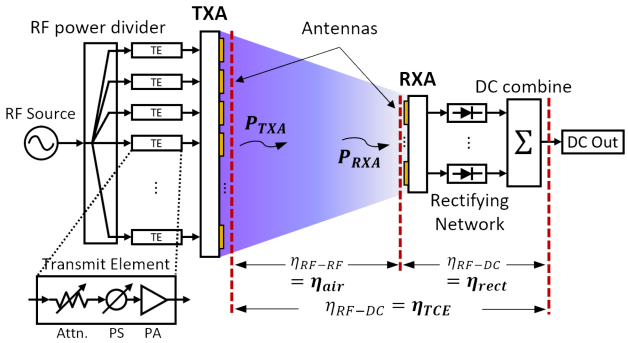

Fig. 1. Conventional MIMO WPT system configuration and its efficiencies.

I. Introduction

INTEGRATED Sensing and Communications (ISAC) is emerging as a key technology for 6G wireless networks, ranging from small sensors and Internet of Things (IoT) devices to vehicles, and beyond. ISAC integrates communication and sensing capabilities, enabling applications, such as wireless brain–computer interfaces, accurate indoor localization, extended reality, energy harvesting, and beyond [1], [2], [3], [4]. Notably, multiple-in–multiple-out (MIMO) wireless power transfer (WPT) technology using radio frequency has emerged as one of the critical technology for ISAC applications, enabling power delivery through air over long distances by sensing and focusing the target [5], [6], [7]. By controlling electromagnetic (EM) waves, WPT allows efficient power transmission in various applications.

One of the key parameters for evaluating a WPT system is the RF-to-RF efficiency, commonly referred to as the power transfer efficiency (PTE), which is defined as the ratio of received RF power to transmitted RF power [8]. Fig. 1 well shows the conventional WPT system configuration, where η_{air} indicates the PTE. Recent research has focused on developing various techniques to enhance PTE [8], [9], [10], [11], [12].

However, near-field (NF) EM effects are becoming increasingly significant in ISAC. The use of large-scale antenna arrays, known as *(Massive) MIMO*, is expected to play a crucial role. As ISAC systems operate at higher frequencies, the combination of Massive MIMO and high operational frequencies will intensify NF EM effects. In these NF environments, a nonuniform power distribution is observed across the receiver array (RXA) elements. Consequently, simply optimizing the RF power can lead to a substantial drop in actual dc output, due to the rectifier behavior. Therefore, it is essential to expand the focus to optimize the received dc power, which inherently involves the rectifier stage η_{rect} to the air propagation stage η_{air}. Research works, such as [13], [14], and [15], share the basic concept, but these approaches have limitations in more practical WPT systems, such as diverse array configurations, arbitrary located receivers, and various rectifier designs.

Especially, mathematical modeling of the rectifier behavior is a complicated work, considering its integration with η_{air} stage models. Modeling the rectifier behavior in various ways were proposed [15], [16], [17], [18], [19]; however, existing formulations are often both complex and inaccurate compared to measured data, making the optimization problem more difficult and less reliable. Therefore, a more accurate yet simpler rectifier modeling approach is required—one that closely matches the

Received 9 May 2025; accepted 5 June 2025. Date of publication 9 June 2025; date of current version 1 December 2025. This work was supported in part by the Institute of Information & Communications Technology Planning & Evaluation (IITP), Korea government (MSIT), through Advanced and Integrated Software Development for Electromagnetic Analysis under Grant 2019-0-00098. *(Corresponding author: Sangwook Nam.)*

Young-Seok Lee, Taeyeong Yoon, Jungsuek Oh, and Sangwook Nam are with the Institute of New Media and Communications (INMC) and the Department of Electrical and Computer Engineering (ECE), Seoul National University, Seoul 08826, South Korea (e-mail: ryanlee@snu.ac.kr; taeyeong.yoon@snu.ac.kr; jungsuek@snu.ac.kr; snam@snu.ac.kr).

Young Jin Song and Sun K. Hong are with the School of Electronic Engineering, Soongsil University, Seoul 06978, South Korea (e-mail: syj1825@soongsil.ac.kr; shong215@ssu.ac.kr).

Digital Object Identifier 10.1109/LAWP.2025.3578089

measured data. To address this need, we propose a measured data-based fitting method.

In summary, this letter proposes the maximization of the received dc power while constraining the total transmitted RF power, which is equivalent to optimizing the transmission-conversion efficiency (TCE), η_{TCE}, as well defined in [13]. The proposed scenario focuses on an optimized rectifier for fixed-load resistance in MIMO WPT, although the methodology is applicable to diverse scenarios regardless of specific applications. A simpler yet more accurate rectifier fitting method is employed to represent the rectifier behavior, avoiding complex mathematical formulations.

The rest of this letter is organized as follows. Section II introduces the main methodology. Section III presents the simulated and measured results. Finally, Section IV concludes this letter.

II. Optimization Procedure

Fig. 1 illustrates a conventional WPT architecture, in which each transmit element within the transmitter array (TXA) is individually controlled in terms of magnitude and phase. The received signals at the RXA are rectified and combined, ultimately yielding the desired dc output power.[1] The WPT system assumed in this letter considers a practical scenario with the following simplifications.

1) All rectifiers are individually optimized and identical.
2) DC power is combined ideally (all power outputs are combined without any losses).

A. RF–RF Optimization

Consider a MIMO WPT system with M transmit antennas and N receive antennas. The channel state information between the TXA and RXA is set as $\mathbf{G} \in \mathbb{C}^{N\times M}$ and $\mathbf{x}_t \in \mathbb{C}^{M\times 1}$ denote the transmit signal vector. Since the problem formulation is based on PTE optimization (hereafter opt.), this can be expressed as follows [20]:

$$\begin{aligned} \max_{\mathbf{S}} \quad & Q_{RF} := \mathrm{tr}\left(\left(\mathbf{GSG}^H\right)/Z\right) \\ \text{subject to} \quad & \mathrm{tr}(\mathbf{S})/Z \le P_t, \quad \mathbf{S} \succeq 0 \end{aligned} \tag{1}$$

where $\mathbf{S} = \mathcal{E}[\mathbf{x}_t\mathbf{x}_t^H]$ is the transmit covariance matrix, Z is the impedance, and P_t is the total transmit power constraint. Since Q_{RF} is the sum of received RF power at the N receivers, this convex problem optimizes the sum of received RF powers with the transmission RF power fixed at P_t, which is a same problem as optimizing the PTE. This is a typical linear convex optimization problem of $\mathbf{S}$, which guarantees the global optimum.

B. Rectifier Fitting Model

Fig. 2(a) shows the typical half-wave rectifier designed for this letter using an HSMS-2860 Schottky diode, operating at 5.64 GHz and 420 Ω load and designed with advanced design system. Fig. 2(b) illustrates the measured data points of the rectifier, collected from 0 dBm to 30 dBm.[2]

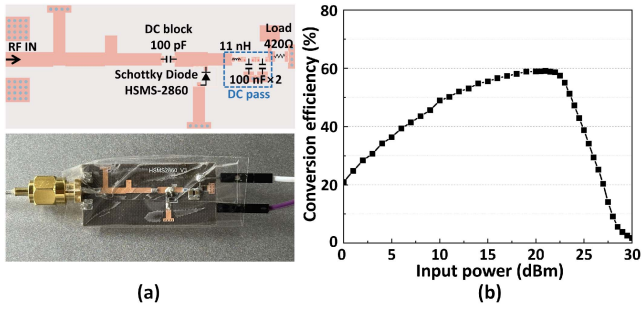

Fig. 2. (a) Conventional half-wave rectifier designed for this work and (b) its measured power conversion efficiency.

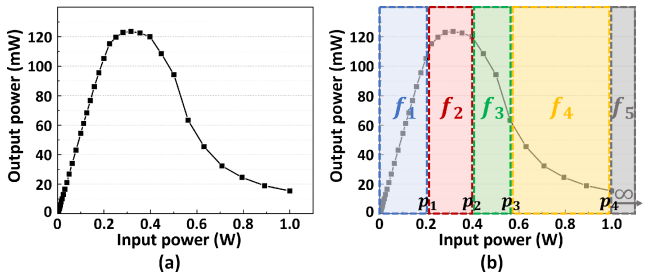

Fig. 3. (a) Rectifier behavior in watts-to-watts and (b) piecewise-defined function based on its convexity.

For a calculable form, the rectifier data in Fig. 2(b) are converted into a watts-to-watts relationship, as shown in Fig. 3(a).[3]

However, the resulting curve is complex to be represented by a single formulation; therefore, it can be divided into several piecewise functions. Fig. 3(b) shows the piecewise-defined function, where all five segments are used, given as follows:

$$P_{\mathrm{DC}} = f(P_{\mathrm{RF}}) = \begin{cases} f_1 & (\text{linear: affine}) \\ f_2 & (\text{quadratic: concave}) \\ f_3 & (\text{cubic: concave}) \\ f_4 & (\text{exponent: convex}) \\ f_5 & (\text{set as '0'}). \end{cases} \tag{2}$$

Then, an additional optimization that minimizes the root-mean-square error between each f_i and the measured data were processed, by selecting the appropriate coefficients.

C. RF-dc Optimization

Now the $f(\cdot)$ is added at (1), where the problem is

$$\begin{aligned} \max_{\mathbf{S}} \quad & Q_{DC} := \sum f\left(\mathrm{diag}\left[\left(\mathbf{GSG}^H\right)/Z\right]_i\right) \\ \text{subject to} \quad & \mathrm{tr}(\mathbf{S})/Z \le P_t, \quad \mathbf{S} \succeq 0. \end{aligned} \tag{3}$$

which becomes complex due to the nonconvexity of the rectifier function, $f(\cdot)$. Unlike the convex optimization problem in (1), formulating an optimization problem that guarantees a global optimum is challenging. Therefore, this letter proposes the use of a global optimization solver: mixed-integer nonlinear programming (MINLP) solver. This is more suitable since the $f(\cdot)$ was simply formulated.

[1] While various methods exist for dividing or combining RF or dc signals, the figure illustrates the most conventional and simple one.

[2] This letter employs a half-wave rectifier, which is the simplest and least efficient type. This choice demonstrates that the proposed method supports practical WPT scenarios where any type of rectifier can be used. Moreover, TCE can be further improved when more advanced rectifiers are employed.

[3] The load in this letter is fixed at 420 Ω, as this value was optimized during the rectifier design itself.

Algorithm 1: Global Optimization Procedure.

- Variable: $\mathbf{S}$.
- Objective: $\sum_i f_{\text{rect}}(p_i)$. here, $p_i = [\mathbf{GSG}^H)/Z]_i$.
- Constraint: Transmitted total RF power; $P_{\text{const}}^{\text{TXA}}$.

Step 1: MINLP Formulation. Start from (3).

$$y_i = f_k(p_i) \;\text{ if }\; \delta_{i,k} = 1, \quad \sum_{k=1}^{4} \delta_{i,k} = 1, \quad \delta_{i,k} \in \{0,1\}.$$

Here, $f_5(\cdot)$ is set to 0 or ignored beyond p_4.

Step 2: Warm Start with RF–RF. Evaluate the initial solution $\mathbf{S}^{(\text{init})}$; compute LB $= \sum_i f_{\text{rect}}\big(p_i(\mathbf{S}^{(\text{init})})\big)$ as a feasible starting point.

Step 3: Global Solver Execution. Call MINLP solver:

1) **Branch and Bound (BB):** Recursively split binary $\delta_{i,k}$ constraints;
2) **Relaxation:** Use convex relaxations to obtain UB;
3) **Pruning:** Discard branches with UB $\leq$ LB;
4) **Feasible Solutions:** Update LB for every iteration.

Continue until global gap $< \epsilon$.

Step 4: Optimization End. Return the final $\mathbf{S}^*$ that maximizes $P_{\max}^{\text{RXA}} = \sum_i f_{\text{rect}}(p_i^*)$.

Step 5: Output. find $\mathbf{x}_t^*$ from $\mathbf{S}^*$ by eigenvalue decomposition [20].

The algorithmic process is summarized in Algorithm 1. For each receiver i, binary variables $\delta_{i,k} \in \{0,1\}$ are introduced to indicate the segment in which p_i lies, subject to the constraint $\sum_k \delta_{i,k} = 1$. The $\mathbf{S} \succeq 0$ satisfies $\text{tr}(\mathbf{S}) \leq P_{\text{const}}^{\text{TXA}}$, which ensures a feasible power budget by limiting the total transmitted RF power. Combining these conditions results in a mixed-integer semidefinite programming formulation. Next, a PTE opt. problem, as described in (1), is solved to obtain an initial feasible beamformer $\mathbf{S}^{(\text{init})}$, for a warm-start lower bound (LB).[4] Subsequently, a global mixed-integer nonlinear programming (MINLP) solver (e.g., BARON or SCIP) is employed, combining the branch-and-bound (BB) framework with convex relaxations to minimize computational complexity. The procedure terminates once the global optimality gap falls below a predefined tolerance ϵ, returning an optimal $\mathbf{S}$ for the piecewise rectifier model. Then, TCE (η_{TCE}) can be written as follows:

$$\eta_{\text{TCE}}\,(\%) \equiv \left(P_{\max}^{\text{RXA}} \;/\; P_{\text{const}}^{\text{TXA}}\right) \times 100 \tag{4}$$

where $P_{\text{const}}^{\text{TXA}}$ denotes the constrained transmitted RF power from the TXA and $P_{\max}^{\text{RXA}}$ represents the optimized received dc power at the RXA.

III. Simulation and Experimental Results

A. Simulation Results

A MATLAB simulation operated by AMD Ryzen 7 5800X processor was conducted. Simulation assumes free-space environment based on antenna patterns by channel calculation, well described in [8]. Fig. 4 shows the TCE optimized results as the size of TXA and RXA changes when transmitted RF power of 20 W, face-to-face, and distance of 0.5 m. Fig. 4(a) shows the

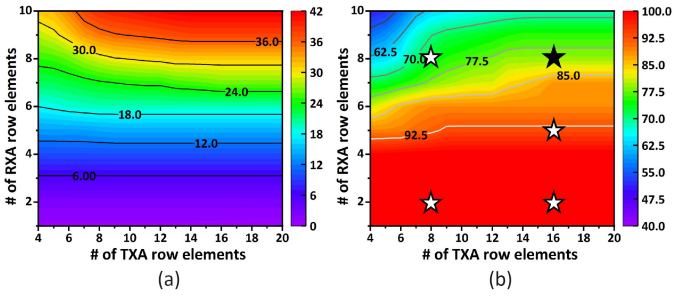

Fig. 4. Contour map by TXA and RXA size when transmitted RF power is 20 W with a distance of 0.5 m. (a) η_{TCE}. (b) η_{RUE}.

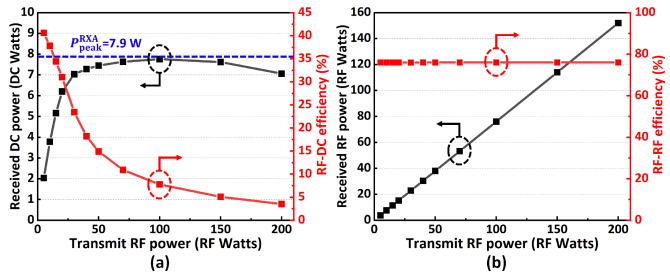

Fig. 5. Received power plot by varying the transmitted RF power: (a) received dc power. (b) RF power.

TCE, where it increases in the vertical direction simply because more receiver antenna elements can receive power. Fig. 4(b) shows the contour plot of "Receiver Utilization Efficiency," which is defined in this letter as

$$\eta_{\text{RUE}}\,(\%) \equiv \left(P_{\text{received}}^{\text{RXA}} \;/\; P_{\text{peak}}^{\text{RXA}}\right) \times 100 \tag{5}$$

where $P_{\text{peak}}^{\text{RXA}}$ represents the maximum possible dc power limit from the RXA, obtained by multiplying the number of RXA elements by the rectifier's peak dc power, while $P_{\text{received}}^{\text{RXA}}$ denotes the total received dc power. Therefore, the RUE means the RXA aperture usage amount. For small RXAs, all rectifiers can achieve peak performance, which RXA aperture is fully used. However, in large RXAs the RUE drops, showing that some antennas are not being utilized.

To demonstrate specific simulation scenarios, suitable sizes for the TXA and RXA must be selected. Based on the contour results shown in Fig. 4(b), five diverse TXA/RXA pairs were chosen (marked by star symbols), covering a range from small to large, with the 16 $\times$ 16 TXA and 8 $\times$ 8 RXA specifically selected as a "reference pair" (black star) suitable for the MIMO scenario.[5] Fig. 5 shows the received power as the transmitted RF power increases from 5 W to 200 W for the "reference pair." Fig. 5(a) clearly illustrates that the received dc power nearly saturates at $P_{\text{peak}}^{\text{RXA}}$, while Fig. 5(b) indicates a linear increase in RF power due to the absence of constraints on the received RF power.

Fig. 6 shows the received RF and dc power as a function of distance for both optimization methods, with a fixed transmitted RF power of 20 W across five different TXA/RXA pairs. The solid line represents the PTE opt. results, while the dashed

[4]Starting from the RF–RF optimal solution significantly shortens the calculation, as global optimization requires a high number of trials.

[5]Less than 1 s to optimize the PTE, while over 3 min took for TCE using "reference pair." MATLAB codes were executed on the CPU.

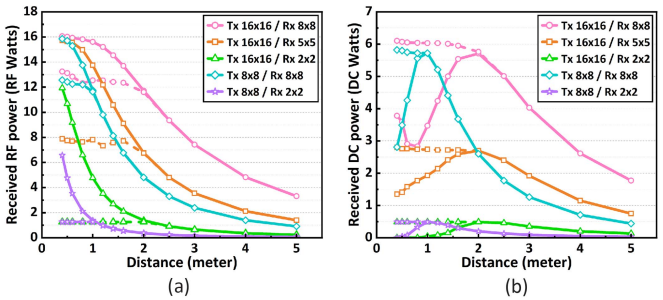

Fig. 6. Received RF and dc power versus distance by different size types, using RF–RF (solid) and RF-dc (dash) optimization: (a) RF and (b) dc.

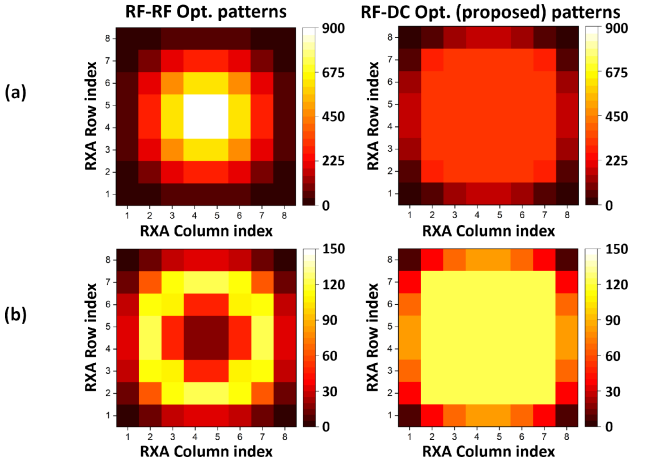

Fig. 7. Heatmap of received power at 8 × 8 RXA by 16 × 16 TXA at 0.5 m distance. (a) Received RF power in mW and (b) received dc power in mW.

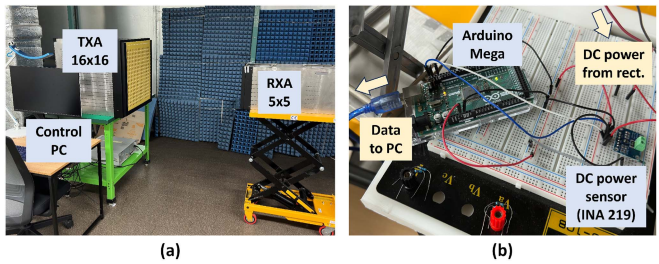

Fig. 8. Measurement setup: (a) 16 × 16 TXA and 5 × 5 RXA and (b) dc power measure setup with Arduino Mega and power sensor.

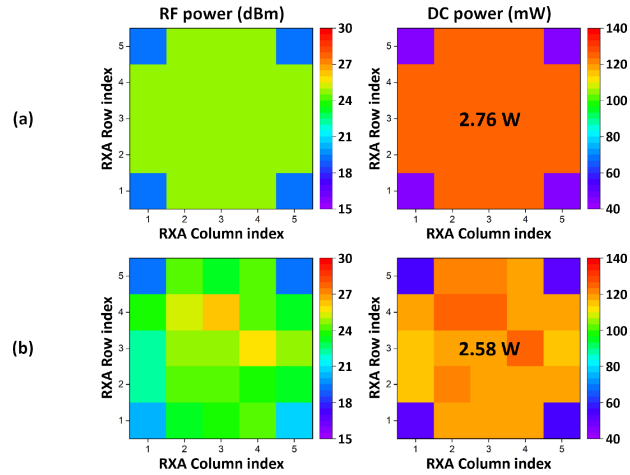

Fig. 9. Heatmap of RF and dc received power distribution of 5 × 5 RXA by 16 × 16 TXA at 0.5 m distance. Result of the proposed optimization: (a) simulated and (b) measured.

line corresponds to the proposed TCE opt. results, which fully achieves higher dc power by directly accounting for the rectifier's characteristics. The results clearly indicate that efficiency decreases as the RXA size becomes smaller. Fig. 7 shows a specific example of the received power distribution for the "reference pair" at 0.5 m, which distance showed the clear difference between RF and dc power, as shown in Fig. 6(b), and also unified with the previous simulation scenarios. It clearly demonstrates that TCE opt. effectively maximizes the peak dc power at the receiver. Since this scenario was selected to highlight MIMO effectiveness, the outer region of the large RXA (8 × 8) does not reach its optimal state, which η_{TCE} decreases as the RXA size grow. The received dc power for PTE and TCE opt. were 3.60 W and 5.96 W, respectively, indicating a significant improvement of 65.6%. Moreover, the calculated η_{TCE} was 18.0% and 29.8%, respectively, underlining the effectiveness of the proposed method in maximizing dc power, particularly in MIMO systems, compared to conventional PTE opt.

B. Measurement Results

Fig. 8 shows the MIMO WPT prototype setup used for measurements [9], [21]. The transmitter operates at 5.64 GHz and includes 256 LP patch antenna elements with 0.6λ element spacing, which can individually deliver RF power up to 1 W. Each individual transmit module contains an antenna, a 7-bit attenuator up to 31.75 dB attenuation, and a 4-bit phase shifter with a resolution of 22.5°. A same antenna with TXA was used for RXA, having size of 5 × 5. Fig. 9(a) and (b) presents the simulated and measured results for a face-to-face scenario at a distance of 0.5 m. The received RF power was measured using a spectrum analyzer, while the dc power was measured using a power sensor (INA 219) connected to an Arduino Mega. The transmitted RF power was constrained to 20 W by controlling the attenuator. The simulated and measured results show a good fit, with the simulated and measured dc power being 2.76 W and 2.58 W, respectively. Considering the well-known challenges in accurately estimating rectifier performance mentioned in the introduction, the results demonstrate strong agreement between simulation and measurement.

IV. Conclusion and Future Works

This letter presents a dc power optimization methodology, which is equivalent to optimizing the TCE and is especially effective in MIMO WPT scenarios for ISAC applications under a certain constraints. In a specific MIMO WPT scenario, a significant 65.6% improvement in TCE compared to conventional PTE optimal was observed through simulations and validated by measurements. These results can be used for such an upper bound for evaluating more practical research works, such as real-time algorithms.

Future work should extend this research to nonideal dc combining and variableload resistance systems under real-world MIMO WPT scenarios (e.g., lowpower IoT or wattscale MIMO applications), considering optimal load resistance determination and compliance with human exposure limits.

REFERENCES

[1] F. Liu et al., "Integrated sensing and communications: Toward dual-functional wireless networks for 6G and beyond," *IEEE J. Sel. Areas Commun.*, vol. 40, no. 6, pp. 1728–1767, Jun. 2022.

[2] M. Z. Chowdhury et al., "6G wireless communication systems: Applications, requirements, technologies, challenges, and research directions," *IEEE Open J. Commun. Soc.*, vol. 1, pp. 957–975, 2020.

[3] W. Saad, M. Bennis, and M. Chen, "A vision of 6G wireless systems: Applications, trends, technologies, and open research problems," *IEEE Netw.*, vol. 34, no. 3, pp. 134–142, May/Jun. 2020.

[4] J. A. Zhang et al., "An overview of signal processing techniques for joint communication and radar sensing," *IEEE J. Sel. Topics Signal Process.*, vol. 15, no. 6, pp. 1295–1315, Nov. 2021.

[5] W. Brown, "The history of power transmission by radio waves," *IEEE Trans. Microw. Theory Techn.*, vol. MTT-32, no. 9, pp. 1230–1242, Sep. 1984.

[6] B. Clerckx, R. Zhang, R. Schober, D. W. K. Ng, D. I. Kim, and H. V. Poor, "Fundamentals of wireless information and power transfer: From RF energy harvester models to signal and system designs," *IEEE J. Sel. Areas Commun.*, vol. 37, no. 1, pp. 4–33, Jan. 2019.

[7] J. Garnica, R. A. Chinga, and J. Lin, "Wireless power transmission: From far field to near field," *Proc. IEEE*, vol. 101, no. 6, pp. 1321–1331, Jun. 2013.

[8] H. Y. Kim, Y.-S. Lee, and S. Nam, "Efficiency bound estimation for a practical microwave and mmWave wireless power transfer system design," *J. Electromagn. Eng. Sci.*, vol. 23, no. 1, pp. 69–74, 2023.

[9] Y.-S. Lee et al., "A design and characterization method of a scalable large transmitting array for wireless power transfer," *IEEE Trans. Microw. Theory Techn.*, vol. 73, no. 6, pp. 3346–3358, Jun. 2025.

[10] Y.-S. Lee, J. Oh, and S. Nam, "Sequential feedback-based phase optimization using hadamard basis for wireless power transfer," in *Proc. IEEE Wireless Power Tech. Conf. Expo.*, Rome, Italy, Jun. 2025.

[11] X. Yang, W. Geyi, and H. Sun, "Optimum design of wireless power transmission system using microstrip patch antenna arrays," *IEEE Antennas Wireless Propag. Lett.*, vol. 16, pp. 1824–1827, 2017.

[12] Y.-S. Lee, J. Oh, and S. Nam, "An effect of time reversal based multiple beacon selection on wireless power transfer performance," in *Proc. IEEE Int. Symp. Antennas Propag.*, Nov. 2024, pp. 1–2.

[13] S. Wan and K. Huang, "Methods for improving the transmission-conversion efficiency from transmitting antenna to rectenna array in microwave power transmission," *IEEE Antennas Wireless Propag. Lett.*, vol. 17, no. 4, pp. 538–542, Apr. 2018.

[14] H. Sun, S. Zhu, R. Ren, H. Zhang, and X. Ma, "Optimization of wireless power transmission under nonuniform incident power density distribution," *IEEE Antennas Wireless Propag. Lett.*, vol. 23, no. 1, pp. 39–43, Jan. 2024.

[15] S. Shen and B. Clerckx, "Beamforming optimization for MIMO wireless power transfer with nonlinear energy harvesting: RF combining versus DC combining," *IEEE Trans. Wireless Commun.*, vol. 20, no. 1, pp. 199–213, Jan. 2021.

[16] T.-W. Yoo and K. Chang, "Theoretical and experimental development of 10 and 35 GHz rectennas," *IEEE Trans. Microw. Theory Techn.*, vol. 40, no. 6, pp. 1259–1266, Jun. 1992.

[17] J. Nahas, "Modeling and computer simulation of a microwave-to-DC energy conversion element," *IEEE Trans. Microw. Theory Techn.*, vol. MTT-23, no. 12, pp. 1030–1035, Dec. 1975.

[18] R. Harrison, "Full nonlinear analysis of detector circuits using Ritz-Galerkin theory," in *Proc. IEEE MTT-S Int. Microw. Symp. Dig.*, 1992, pp. 267–270.

[19] S. Ladan and K. Wu, "Nonlinear modeling and harmonic recycling of millimeter-wave rectifier circuit," *IEEE Trans. Microw. Theory Techn.*, vol. 63, no. 3, pp. 937–944, Mar. 2015.

[20] R. Zhang and C. K. Ho, "MIMO broadcasting for simultaneous wireless information and power transfer," *IEEE Trans. Wireless Commun.*, vol. 12, no. 5, pp. 1989–2001, May 2013.

[21] Y.-S. Lee et al., "LUT-based transmit mode calibration complexity reduction method for wireless power transfer," in *Proc. IEEE Wirel. Power Technol. Conf. Expo.*, Kyoto, Japan, May 2024, pp. 137–141.